WPS5004

Policy Research Working Paper 5004

Forecasting Local Climate for Policy Analysis

A Pilot Application for Ethiopia

Brian Blankespoor
Kiran Dev Pandey
David Wheeler

The World Bank
Environment Department
&
Development Research Group
July 2009

Policy Research Working Paper 5004

Abstract

This paper describes an approach to forecasting future climate at the local level using historical weather station and satellite data and future projections of climate data from global climate models (GCMs) that is easily understandable by policymakers and planners. It describes an approach to synthesize the myriad climate projections, often with conflicting messages, into an easily-interpreted set of graphical displays that summarizes the basic implications of the ensemble of available climate models. The method described in the paper can be applied to publicly-available data for any country and for any number of climate models. It does not depend on geographic scale and can be applied at the subnational, national, or regional level. The paper illustrates the results for future climate for Ethiopia using future climate scenarios projects by 8 global climate models. The graphical displays of nine possible future climate regimes (average temperature, precipitation and their seasonal distribution) for each grid-cell about 50km X 50 km). It also provides the probability associated with each of the nine-climate regimes.

This paper—a product of the Environment Department and Development Research Group of the World Bank—is part of a larger study on the Economics of Adaptation to Climate change in the Environment Department. The study is a partnership of the World Bank which is leading the technical aspects of the study, and the Governments of the United Kingdom, the Netherlands and Switzerland who are funding the study. Additional information and papers from this study can be found at http://WorldBank.org/Environment/EACC. Policy Research Working Papers are also posted on the Web at http://econ.worldbank.org. The author may be contacted at kpandey@worldbank.org.

Forecasting Local Climate for Policy Analysis: A Pilot Application for Ethiopia

Brian Blankespoor
Kiran Dev Pandey
David Wheeler

This paper has been fully or partially funded by the Economics of Adaptation to Climate Change study. The study is a partnership of the World Bank which is leading the technical aspects of the study, and the governments of the United Kingdom, the Netherlands and Switzerland who are funding the study. The Economics of Adaptation is a larger effort in the department to make aid more effective in promoting economic development. Papers in this series are also posted on the Web at http://WorldBank.org/Eenvironment/EACC. Questions about the paper can be addressed to Kiran Dev Pandey at kpandey@worldbank.org.

1. Introduction

This paper describes an approach to local climate forecasting that integrates local weather history and future projections in simple display formats that are useful for policymakers. It draws on historical climate data from weather stations and satellites; projections from climate models (GCMs) linked to global emissions scenarios from the Intergovernmental Panel on Climate Change (IPCC); and a methodology for summarizing stochastic variation in the data. The methodology can translate very large, multidimensional datasets into easily-interpreted formats for all countries at a high level of spatial disaggregation. In this pilot application for Ethiopia, we develop formats for 372 grid squares that cover the whole country; three time periods (1960-2000, 2001-2050, and 2051-2100); eight GCMs[1]; and one IPCC future emissions/climate scenario (A1B). However, we have designed our approach for an arbitrary number of grid squares, periods, GCMs and IPCC scenarios. It can produce a fine-gridded database for multiple periods that covers all countries and incorporates predictions from all available GCMs and IPCC scenarios.

This exercise is primarily designed to serve policymakers, public investment planners and other actors whose decisions must necessarily balance a host of technical, economic, political and social concerns. For these people, the future impact of global warming is one factor among many that must be considered. At the same time, appropriate decisions require an approach that captures all the relevant dimensions of future climate forecasts, at least to a first approximation. This paper describes and implements such an approach through a step-by-step process. The remainder of the paper is organized as follows. In Section 2, we provide a general introduction to the

[1] See Appendix 1 for documentation of the eight GCMs.

methodology and describe the steps for implementing it in the Ethiopian case. Section 3 provides illustrations of the results for areas in four Ethiopian regions, and Section 4 concludes the paper.

2. The "Best Fit" Approach to Downscaling

"Downscaling" describes the process by which information from a large, heterogeneous global climate dataset is tailored to local conditions to produce local weather projections. Downscaling has two essential components: a system for benchmarking local-historical weather data, and a system for bridging from these historical data to GCM forecasts. One problem is that GCMs are calibrated at global scale, and individual GCMs may not fit local conditions very well. Another problem is posed by the sheer number of GCMs, which may present very different views of future prospects for a particular area. We need a methodology for judging the "fit" of each GCM to local conditions, and a tractable representation of the uncertainty faced by each area.

We begin with monthly temperature and rainfall data for the period 1961-2000 (henceforth CRU), provided by the Climatic Research Unit of the University of East Anglia, Norwich, UK. The data are gridded to .5°, producing 372 grid squares for Ethiopia. These fine-gridded data combine historical observations from specific weather stations with spatial interpolations that combine information from the weather stations and satellite-based observations. The data enable us to characterize historical climate variation as a bivariate distribution of temperature and rainfall. They also establish a benchmark for tailoring GCM projections to local conditions.

We implement our methodology in the following steps:

2.1 Assignment of reliability weights to the eight GCMs, based on their historical "goodness of fit" to the CRU data

We use R^2's rather than the simple correlation coefficients, because we want to discriminate strongly in favor of the best-fitting GCMs. Our approach is bivariate, because temperature and rainfall are jointly produced by the climate process. To assign reliability weights, we combine fine-gridded historical results for each GCM with monthly temperature and rainfall data for the period 1961-2000 (CRU), provided for Ethiopia by the Climatic Research Unit of the University of East Anglia, Norwich, UK. We compute R^2's between CRU and each of the eight GCMs for temperature and rainfall separately. Each estimate is based on 178,560 observations (monthly during 1961-2000 for 372 Ethiopian grid squares). We add rainfall and temperature R^2's to get a summary measure of explained variation for each GCM, specify the smallest value as the numeraire, and divide it into the others to get relative scores.

2.2 Establishment of forecasting benchmarks for each grid square

We require separate benchmarks for the CRU and each of the GCMs. We establish forecasting benchmarks for each grid square using data for the period 1980-2000 (the most recent year in our CRU dataset). We begin by computing average annual rainfall and temperature for the nine datasets (CRU; 8 GCMs). Then we use a least-squares fit criterion to select the most representative joint monthly distribution of temperature and rainfall. For each variable, we compute squared monthly deviations from median values in each grid square. We calculate yearly sums of squared deviations for each grid square, and then rank the 21 results (1980-2000) separately for temperature and rainfall. We use ranks to ensure robust results, since temperature and rainfall metrics are quire different.

Then we compute squared yearly deviations of ranks from their medians for temperature and rainfall in each grid square; calculate sums of squared deviations (SSD) for each variable; and identify the year with lowest SSD as the benchmark year. By this "two-stage least-squares" criterion, the temperature and rainfall for the benchmark year provide the best bivariate representation for the 21-year dataset in each grid square. The process generates nine benchmark annual datasets – CRU and eight GCMs – for each of the 372 grid squares.

2.3 Generation of benchmarked annual forecast ratios for the GCMs

For each GCM, this entails dividing each observation in each future year by the GCMs counterpart observation in its benchmark dataset (most representative temperature/rainfall among the 21 years in the period 1980-2000). The resulting dataset contains 297,600 ratios (8 GCMs, 372 grid squares, 100 years).

2.4 Computation of GCM-based forecasts from actual historical data

For each GCM, this entails multiplying each yearly ratio (from 2.3 above) in each future year by the counterpart observation in the CRU benchmark dataset (from the most representative temperature/rainfall combination, derived from CRU data for 1980-2000). This procedure serves two goals. It retains the relative changes incorporated in future GCM estimates, and it applies these relative changes to the actual point of historical departure: the benchmark series from the CRU data. This translation step is necessary because the GCMs reflect consistent, global-scale computations but are not designed to accurately reproduce local climate regimes. That is why we have developed R^2-based "goodness-of-fit" scores in the first stage of this process.

2.5 Separation of forecasts into relevant future periods

Selection of intervals within the 100-year forecast range (2001-2100) is essentially arbitrary. For this study, we divide the 21st century into two 50-year intervals (2001-2050; 2051-2100) to provide a simple illustrative template.

2.6 Separation of weather data into scale classes

The GCMs attempt to replicate actual climate patterns by incorporating year-to-year stochastic variation into their forecasts. At the same time, the GCMs incorporate long trends in the annual levels and monthly distributions of rainfall and temperature. For each GCM, each 50-year forecast interval therefore includes widely-varying joint observations on temperature and rainfall. The total forecast variation is compounded by the presence of 8 GCMs. For the scale-separation exercise, we use our calculated yearly temperature and rainfall pairs for each GCM in each future forecast interval. This generates 400 annual totals (8 GCMs; 50 years) for temperature and rainfall for each of 372 grid squares. These reflect anticipated future climate trends as well as broad stochastic variation from year to year. To establish the full domain for variation, we assemble annual observations as follows for each grid square: the first 40 from the CRU data (1961-2000) and the other 800 from the GCM-based forecasts (2 future periods, 50 years in each period; 8 GCMs).

For tractability, we need a simple scheme for characterizing this variation. For this paper, we establish three equal-sized intervals from minimum to maximum values (Low, Medium, High), for rainfall and temperature separately, for the 840 observations in each grid square. Then we assign each annual joint rainfall/temperature observation in each

year (1960-2000; 2001-2050; 2051-2100) to one of nine cells in a 3-3 matrix (reflecting all possible combinations of low, medium and high values for temperature and rainfall).

Now we are ready to develop a simple template for calculating joint incidence probabilities for the two variables in each period. The first step draws on the reliability weights calculated in Step 2.1 of the analysis. In fact, the 8 GCMs are far from equal in their ability to reproduce local climate patterns in Ethiopia. To quantify this difference, we have calculated the R^2-based scores that were previously described. Now we use these scores in an expectational calculus. The intuition here is straightforward: In the two future periods, we cannot assign the same confidence to predictions from different GCMs. Before we assign a GCM-based forecast to one of the nine cells for a grid square, we weight it with the R^2-based score that we have computed for the GCM. In effect, we count an observation from the best-fitting GCM as occurring more frequently than an observation from the numeraire (worst-fitting GCM). The relative frequency is the ratio of a GCMs R^2 score to the numeraire score (for the worst-fitting GCM).

Once the weighted observations are all assigned to the nine cells for each grid square, we calculate the weighted probability for each cell (total cell score/total of all cell scores). We do this for both future periods, as well as for the historical CRU data (here each observation gets unit value in the count, since all observations are deemed equally reliable). The result is an easily-interpreted template for each grid square, which shows the transition in expected Low-Medium-High incidence of temperature/rainfall pairs from actual recent history, to the relatively near future, and then to the distant future. This provides decision-makers with a clear, simple picture of our best evidence on how the

current stochastic distribution of climate events is expected to change during the coming century.

2.7 Selection of representative future monthly forecasts

The procedure summarized in 2.6 provides a view of expected change in annual temperature and rainfall conditions. However, investment planning in agriculture and other sectors will also be sensitive to expected changes in the monthly pattern of temperature and rainfall. So the final challenge is to distill our best guess about future monthly patterns from the huge set of future monthly predictions at our disposal. And we have to do this while preserving the jointness of temperature and rainfall data – they cannot be separated for summary purposes.

We begin by expanding the previously-computed annual totals into monthly distributions, in two steps. First, for annual temperature and rainfall data for each GCM, we compute the ratio of each monthly observation to the corresponding annual mean value. Then we apply these ratios to the forecast annual means produced in Step 2.4. The result is a dataset with 3,571,200 observations (372 grid squares; 8 GCMs; 100 years; 12 months/year). In each grid square, we have nine probabilities (which sum to 100%) assigned to Low-Medium-High combinations of annual temperature and rainfall. For cells with non-zero probabilities, we select representative monthly distributions using a weighted variant of our previously-described approach to benchmarking: Within each of the nine cells in each future period (and grid square), we compute squared monthly deviations from medians for temperature and rainfall for each year and GCM model. We weight the squared deviations by the inverse of the GCMs "goodness-of-fit" score (this assigns lower deviation values to better-fitting GCMs, ceteris paribus), which has the

effect of moving the choice of a representative monthly series toward the better-fitting GCMs). Then we compute annual totals for the weighted squared deviations for temperature and rainfall separately. As before, we calculate cell ranks for the two variables, and perform the second-stage squared-deviations operations on the ranks to get annual scores for each GCM and year. We select the GCM/year which has the lowest score (and is therefore closest to the central tendency in the dataset, by our criteria) and identify the monthly series for that GCM/year as the most representative series for comparative analysis.

2.8 The analysis tableau

The complete tableau has the following elements. Each grid square has nine cells containing incidence probabilities for annual temperature/rainfall totals in each of three periods (past, near future, distant future). Each cell is also assigned a monthly joint series of rainfall and temperature for the past (from the benchmark CRU series that we have already described in 2.2 above), as well as monthly series for the two future periods. This "distillation" still creates a massive dataset (as many as 9 cells, 3 periods, 372 grid squares, although many cells have zero expected incidence. But for any specific grid square (the locus of investment decisions), the template is quite tractable: no more than 9 monthly series for each of 3 periods.

3. Illustrative Results for Ethiopia

Figure 1 provides evidence on historical weather patterns in different parts of Ethiopia. For each indicated grid point, we depict the "best-fit" monthly historical pattern of temperature (above in each pair) and rainfall. The data for each variable are graphed with the same vertical scale at each point, so that relative levels can be

compared. Typical temperatures are much higher at the western and eastern grid points (between 25° and 30° C.) than at the central (highland) point (10° - 15° C.). Both levels and seasonal variations in rainfall are also quite different. The central point has high average rainfall, with a smooth pattern of rise and fall that is approximately centered in July (month 7). The southern and eastern points have very low rainfall, distributed in a bimodal pattern with peaks in the spring and fall. The other two points have sharply single-peaked distributions, peaking in July in the west and August in the north.

Figure 2 presents our benchmark results for weighting GCMs in this exercise. The table presents average R^2 scores for the bivariate relationships between the CRU (historical) rainfall and temperature observations and the corresponding observations from the 8 GCMs (documented in Appendix 1). Each score is computed from monthly observations for 40 years, over 372 Ethiopian grid squares. The best fit ($R^2 = .50$) is provided by GISSA, the AOM model of NASA's Goddard Institute for Space Studies. The worst fit ($R^2 = .10$) is provided by IPSL, the CM4 model of the Institute Pierre Simon Laplace, France. We should emphasize that these results are for Ethiopia only. It is quite possible that the pattern of fit across GCMs is very different for other countries. In any case, we observe stark differences for Ethiopia: The ratio of R^2-scores for best and worst fit is 5:1. We use relative weights computed from the results displayed in Figure 1 in the stepwise "best-fit" exercise described in Section 2.

Figures 3-5 illustrate our projection results for three grid points in Figure 1. As we note in Section 2, our methodology condenses all the GCM information into "best-fit" patterns for three periods: historical (1960-2000), 2001-2050 and 2051-2100. For Figures 3-5, we juxtapose the projections for 2051-2100 (in red) with historical data

(blue). The data are condensed into a nine-cell matrix that includes low, medium and high ranges for annual temperature and rainfall. Figures 3-5 include all cells that actually contain observations in our results. Figure 3, drawn from the southern grid point, includes results for 7 of the 9 possible matrix cells. The cells are ordered by probability. The topmost graphs portray the future scenario with the highest probability (47.6%) at this grid point. Rainfall remains low and roughly bimodal, but the pattern shifts forward by about two months. Projected temperature rises about 2° C, but the change is not constant across the seasons. The maximum difference occurs in spring and summer, while fall temperatures are much closer to the historical pattern.

The other cells in Figure 3, in descending order of probability, indicate preservation of bimodality in rainfall, somewhat higher levels of rainfall, and generally higher peaks in the rainiest months. These patterns are most pronounced in two of the lowest-probability cells (2.8% and 1.5%), which also indicate forward-shifting by about two months. The corresponding temperature results also suggest higher temperatures on average, but the pattern varies considerably. In the second-highest-probability cell (22.8%), projected temperatures are much closer to historical patterns than in the highest-probability cell. The other cells reveal the same kind of variation.

Figures 4 and 5 reveal similar variety in the levels and seasonal distributions of rainfall and temperature. The central Ethiopian point in Figure 4 has much less skew in its scenario probabilities than the southern point. It also displays marked variation in seasonal rainfall patterns: a pronounced shift forward toward a fall peak in the highest probability cell (36.3%); a shift backward toward a spring peak in the second-probability cell (31.1%), and a shift toward steeply-peaked bimodality in one of the lower-probability

cells (7%). Projected temperatures in the central (highland) cell remain low by Ethiopian standards, but they are persistently 1° - 2° C. higher than historical figures.

Figure 5 displays results for the eastern grid point, and they are similar to those for the southern point in Figure 3. Figure 6 provides a more detailed representation for the western point, presenting the entire 9-cell matrix for the three periods. The use of a constant low-medium-high breakdown across all three periods enables us to see the pattern of climate transition clearly, along with shifts in seasonal patterns. Rainfall is in the left column for each pair. In the historical period (1960-2000), almost all of the observations are in low-temperature cells, while rainfall is more broadly distributed (low rainfall 12.5% probability; medium rainfall 55.0%; high rainfall 30%). The period 2001-2050 witnesses a marked stretching of the distribution, with observations in 8 of the 9 matrix cells. Temperatures begin extending into the medium and high regions, while rainfall remains varied and seasonal patterns exhibit significant differences across cells. By the period 2051-2100, all of the low-temperature cells have dropped out while rainfall remains highly varied. The highest-probability cell (56.0%) has high temperature and medium rainfall, while the second-probability cell (27.5%) has medium temperature and medium rainfall. The seasonal pattern of rainfall in the two high-probability cells has roughly the same shape, peaking in the fall. The seasonal rainfall pattern is clearly different in some of the lower-probability cells.

4. Summary and Conclusions

In this paper, we have developed an Ethiopian illustration for a downscaling methodology that summarizes information from historical climate data and future projections from 8 global climate models. This method can be applied to publicly-

available data for any country, and for any number of climate models. No matter how many models are included, the method will summarize information for each grid point in the nine-cell matrix portrayed in our Ethiopian illustrations. The information is computed for each square in a fine-gridded map (372 squares for Ethiopia alone). It includes the relative likelihood of future climate regimes, along with associated changes in average temperature and rainfall, and the seasonal distributions of those variables. We believe that this spatial information is sufficiently disaggregated to be useful for local planners and policymakers. At the same time, our method is invariant to scale. After aggregation of grid cells, it can be applied to national subregions, nations, or entire regions. We therefore believe that it can provide a generally-useful tool for policymakers and planners who need to understand the basic implications of the myriad climate projections that are now available.

Figure 1: Monthly Temperature and Rainfall in Five Ethiopian Regions

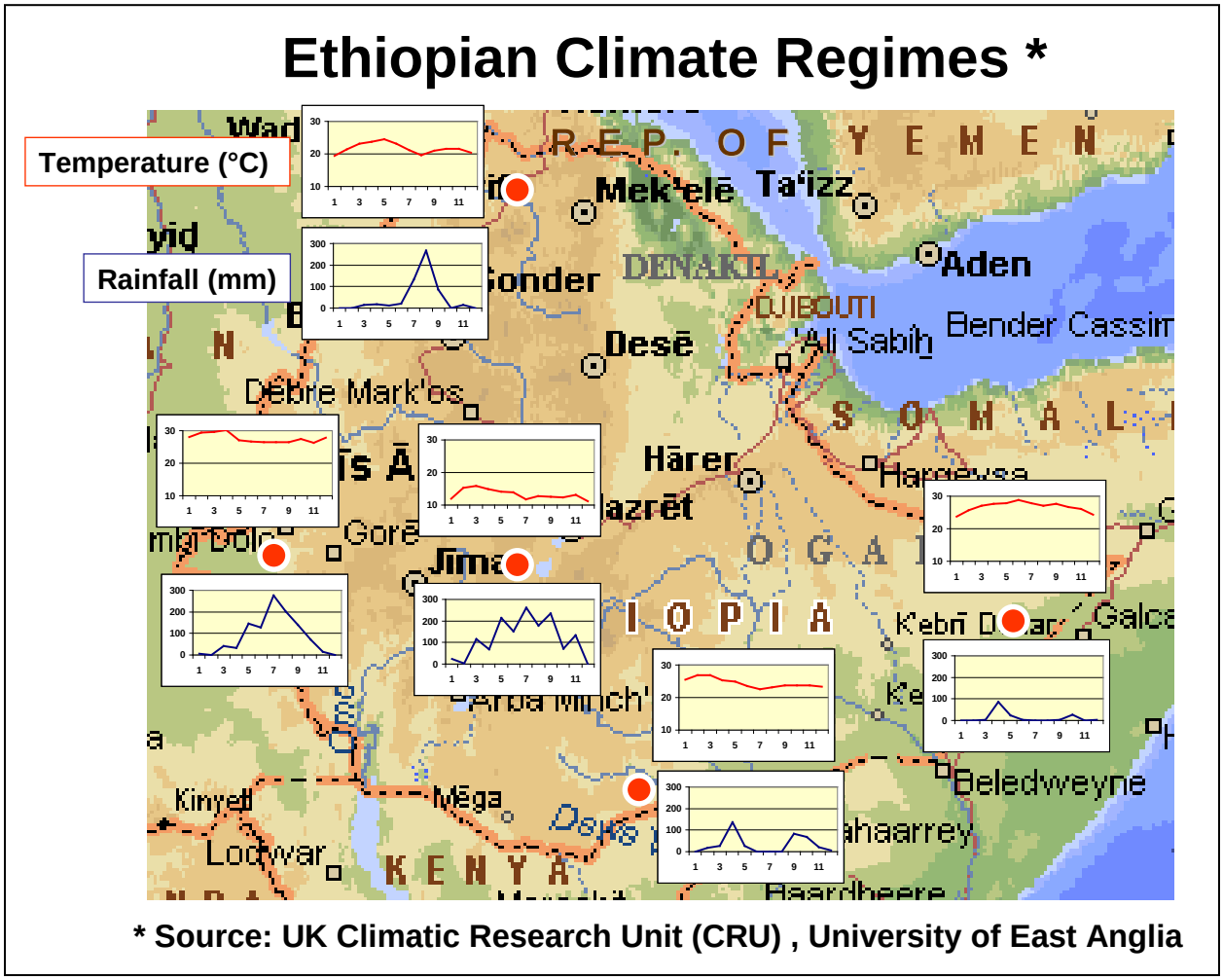

*** Source: UK Climatic Research Unit (CRU) , University of East Anglia**

Figure 2: Relative Fit to CRU Data: 8 Global Climate Models

GCM Fit to CRU

Assign reliability weights to the eight GCM's, based on their historical "goodness of fit" to the CRU data (R^2).

Model	Weight
GISSA	0.50
GFDL	0.38
CCCMA	0.37
UKMOHAD	0.34
MIROC	0.33
MIUBE	0.15
INM	0.12
IPSL	0.10

Observations

178,560

372 Grid Cells

X

40 Years

X

12 Months/Year

Figure 3: Present and Future Climate in Southern Ethiopia

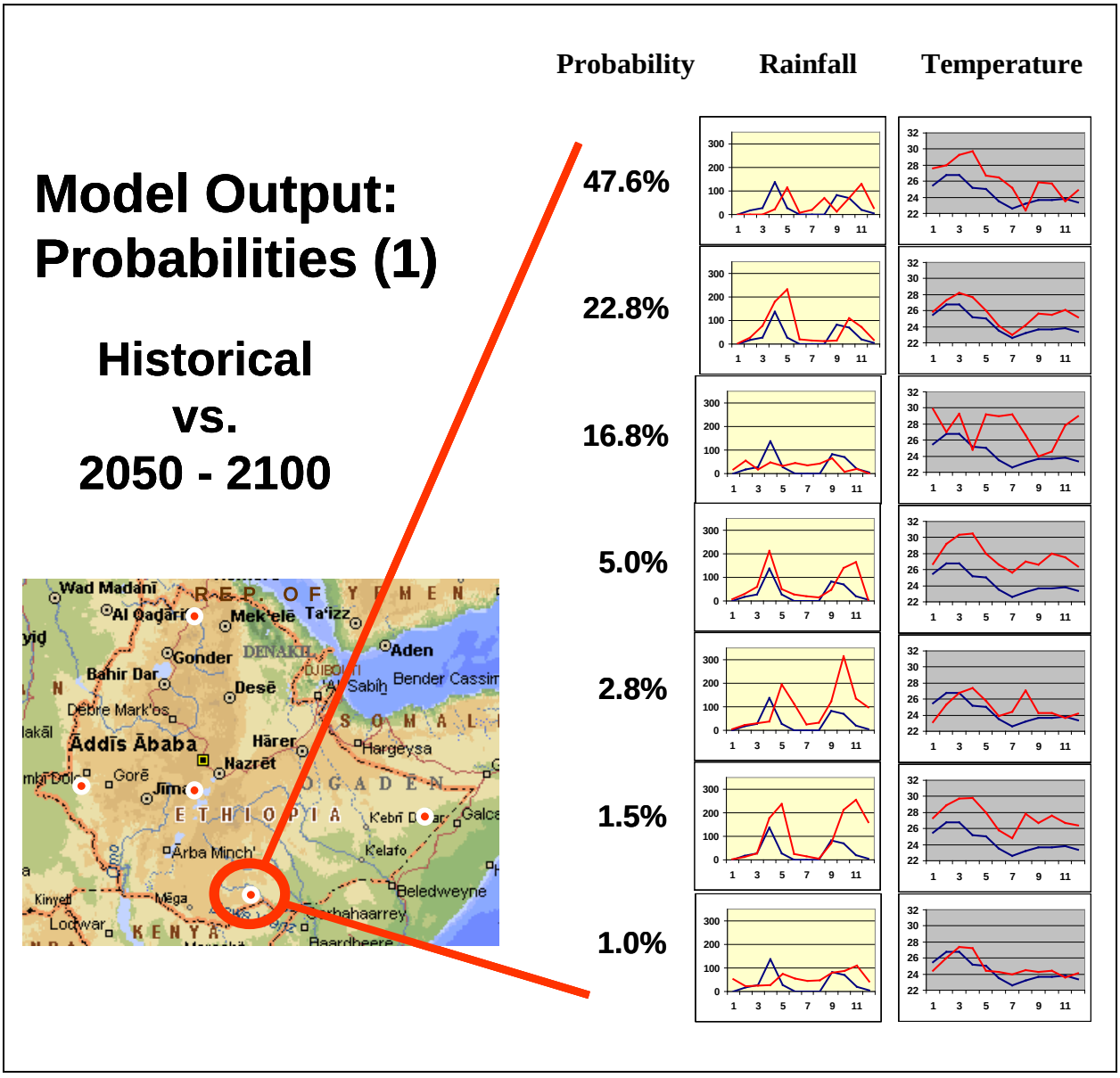

Figure 4: Present and Future Climate in Central Ethiopia

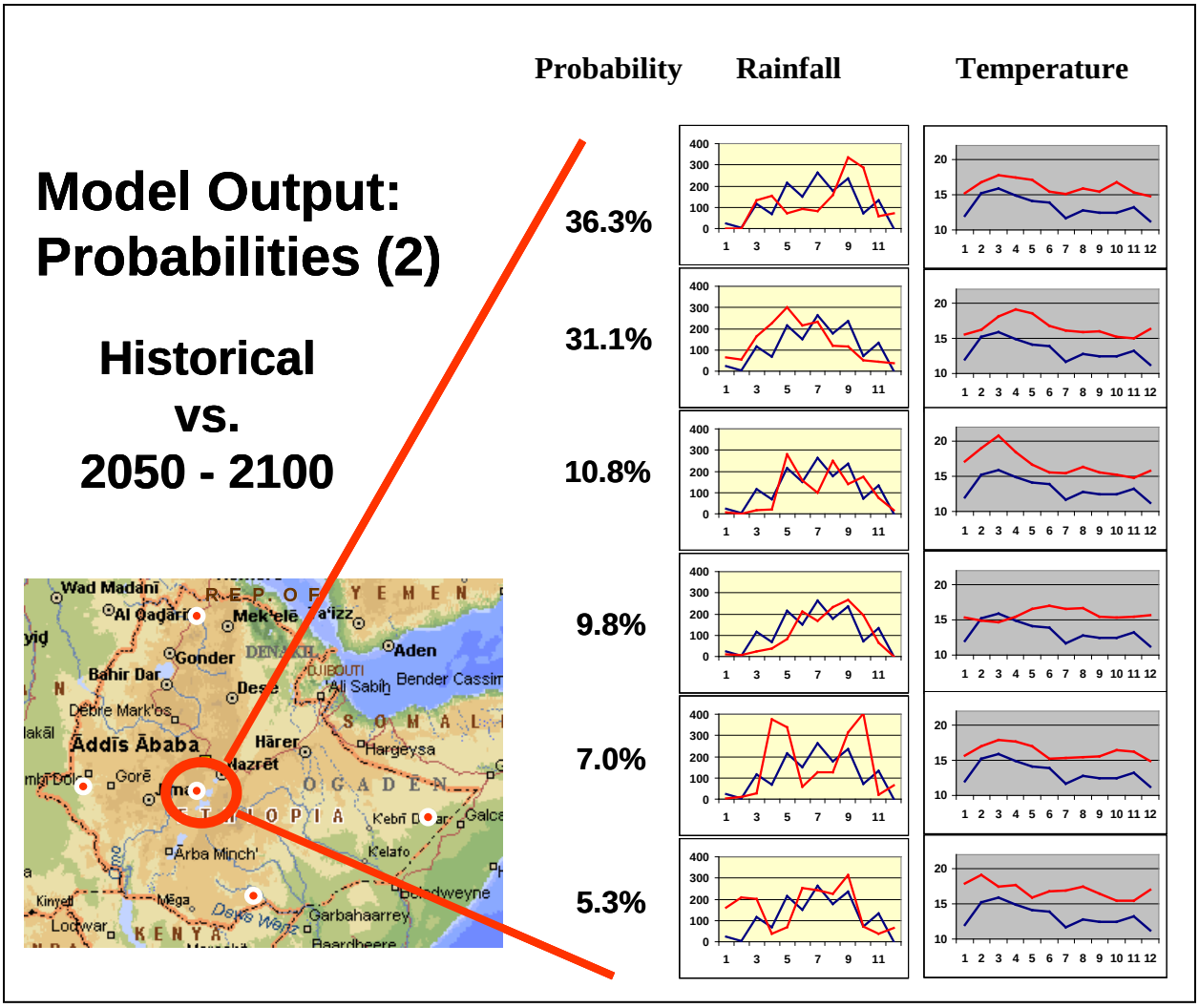

Figure 5: Present and Future Climate in Eastern Ethiopia

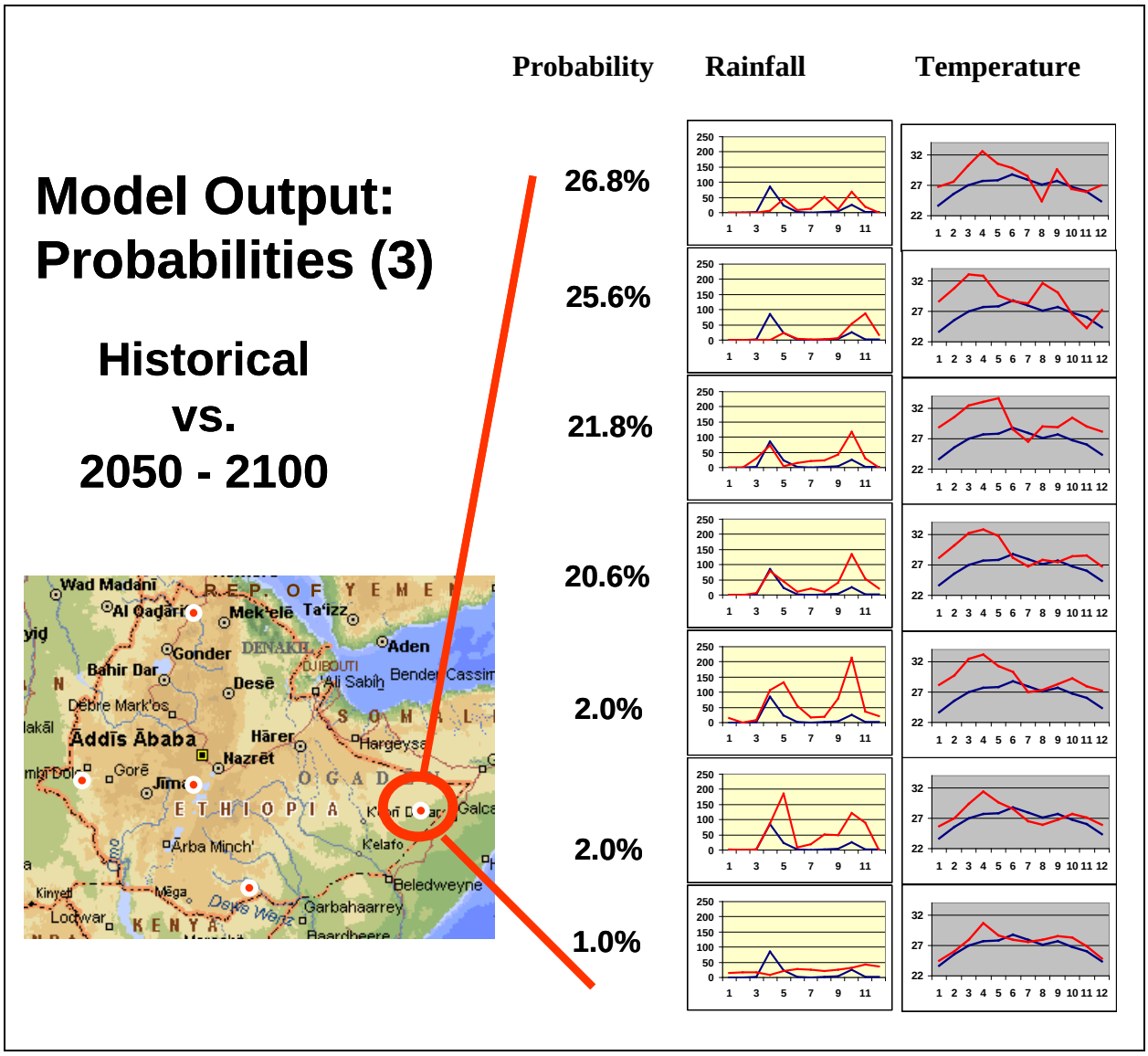

Figure 6: Present and Future Climate in Wester~~mn~~n Ethiopia

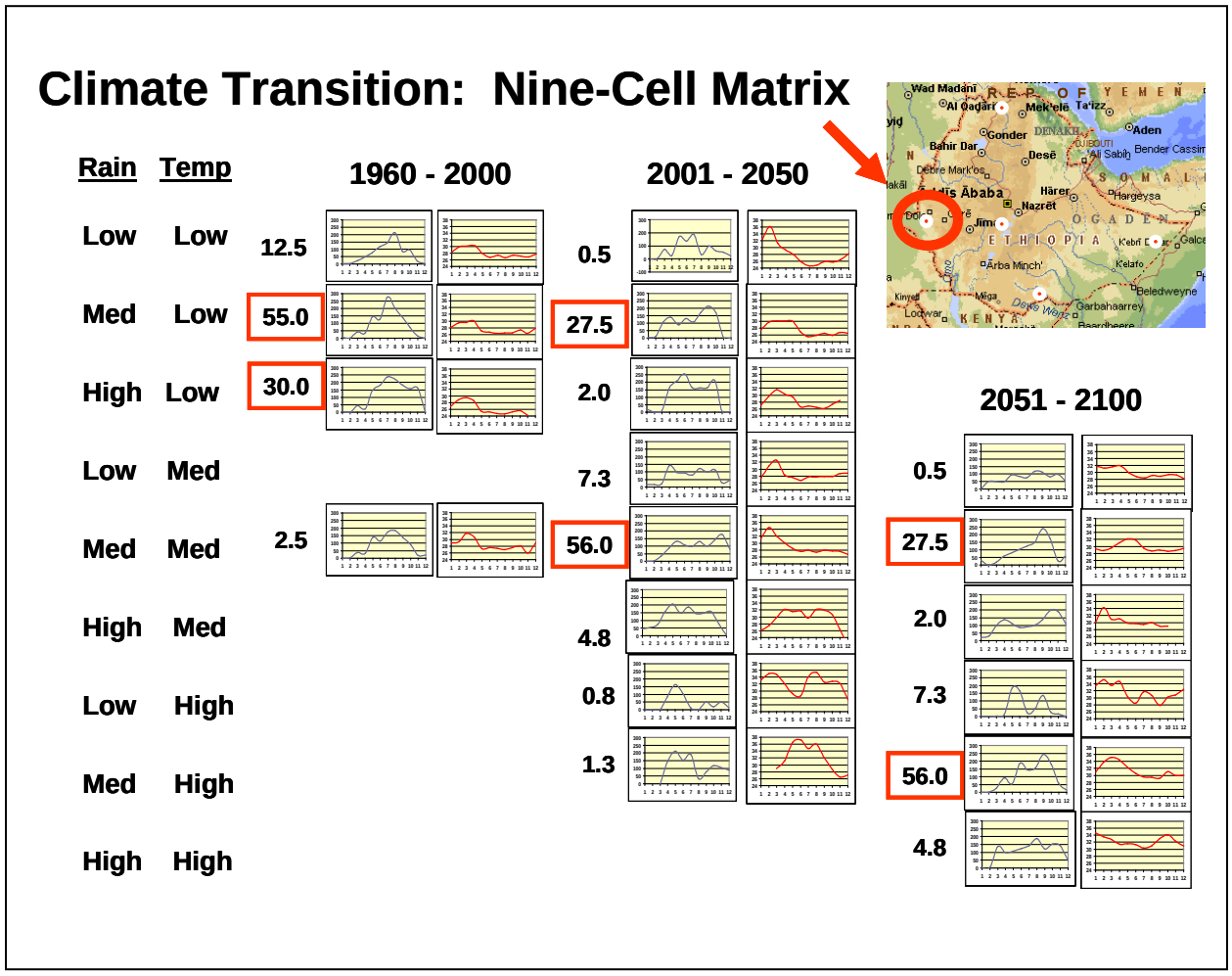

Appendix 1: CRU and GCM Sources

Historical Data: 1961-2000

CRU: UK Climatic Research Unit, University of East Anglia, UK
http://www.cru.uea.ac.uk/

GCM Data: 1961-2100

GFDL: Geophysical Fluid Dynamics Laboratory, NOAA, USA
Model Name: CM2
http://www.ipcc-data.org/ar4/model-GFDL-CM2-change.html
http://www.ipcc-data.org/ar4/model-GFDL-CM2_1-change.html

CCCMA: Canadian Centre for Climate Modeling and Analysis: GCM3
Model Name: GCM3
http://www.ipcc-data.org/ar4/model-CCCMA-CGCM3_1-T63-change.html
http://www.ipcc-data.org/ar4/model-CCCMA-CGCM3_1-T47-change.html

GISSA: NASA Goddard Institute for Space Studies (NASA/GISS), USA
Model name: AOM
http://www.ipcc-data.org/ar4/model-NASA-GISS-AOM-change.html

INM: Institute of Numerical Mathematics, Russian Academy of Science, Russia.
Model name: CM3.0
http://www.ipcc-data.org/ar4/model-INM-CM3-change.html

IPSL: Institut Pierre Simon Laplace, France
Model Name: CM4
http://www.ipcc-data.org/ar4/model-IPSL-CM4-change.html

MIROC: CCSR/NIES/FRCGC, Japan
CCSR: Center for Climate System Research, University of Tokyo
NIES: National Institute for Environmental Studies, Japan
FRCGC: Frontier Research Center for Global Change, Japan Agency for Marine-Earth Science and Technology (JAMSTEC)
Model Name: MIROC3.2
http://www.ipcc-data.org/ar4/model-NIES-MIROC3_2-HI-change.html
http://www.ipcc-data.org/ar4/model-NIES-MIROC3_2-MED-change.html

MIUBE: Meteorological Institute of the University of Bonn (Germany), Institute of KMA (Korea), and Model and Data Group.
Model Name: ECHO-G
http://www.ipcc-data.org/ar4/model-CONS-ECHO-G-change.html

UKMOHAD: Hadley Centre for Climate Prediction and Research, Met Office, UK

Model Name: HadCM3
http://www.ipcc-data.org/ar4/model-UKMO-HADCM3-change.html